Chapter 7

Pressure Seals—Interactions with Organic Matter, Experimental Observations, and Relation to a "Hydrocarbon Plugging" Hypothesis for Pressure Seal Formation

Jean K. Whelan
Lorraine Buxton Eglinton
Woods Hole Oceanographic Institution
Woods Hole, Massachusetts, U.S.A.

Lawrence M. Cathles III
Cornell University
Ithaca, New York, U.S.A.

ABSTRACT

Organic geochemical characteristics diagnostic of pressure seals have been determined for two wells in the Moore-Sams field of the Tuscaloosa trend, Louisiana Gulf Coast (Mix and Bizette wells) and one well penetrating a much weaker pressure transition zone of the Anadarko basin, Oklahoma (Weaver well). Preliminary data suggest these characteristics of organic matter in zones of pressure seals: a rapid increase in vitrinite reflectance near the top of the pressure seal; fractionation of bitumens through the pressure seal with a gradual change from lighter to heavier n-alkanes with increasing depth in the pressure seal; a buildup of hydrocarbons just beneath the pressure seal; and an enhancement of asphalt (or asphaltene) throughout the general zone of the pressure seal. For all three wells, very tight associations of carbonate cements, fine pyrite, asphaltenes, and micrinite (generally considered to be a residual product of hydrocarbon generation) were observed in the general zone of pressure seals, suggesting that interactions of organic and inorganic materials may be required for pressure seal formation and maintenance, even in fairly organic lean wells such as Weaver. A sharp jump in thermal maturity, as measured by vitrinite reflectance, occurs at the top of the Mix pressure transition zone. Maturity levels below the seal reach gas thermal window levels, suggesting that gas formation within and below the (seal) zone is contributing both to overpressuring and sealing of pressure seals investigated here. It is proposed that all these observations can be accommodated if the pressure drop across the seal pressure transition zone causes separation of oil and gas and deposition of asphalt from the upward-

streaming oil/gas that carried them from sources at greater depths. Permeability is reduced through a combination of asphalt hydrocarbon plugging, inorganic alteration, and (most important) gas-water capillary effects.

BACKGROUND AND INTRODUCTION

Recent observations and measurements have shown that large cells, or fluid compartments, persist in the subsurface that remain out of hydrostatic equilibrium with adjacent sedimentary rocks over geologic time (Bradley, 1975; Powley, 1980, 1990; Hunt, 1990; Weedman et al., 1992). Furthermore, some mechanisms of pressure seal formation and maintenance appear to have a significant geochemical component as described in several contributions in the current volume.

Throughout this paper, the term *pressure seal* is used to mean a zone in the subsurface of inferred extremely low permeability that maintains a measurable water pressure anomaly and is used synonymously with *pressure transition zone.*

The purpose of this research was to clarify the role of sedimentary rock organic matter, oil, and gas with respect to three aspects of pressure cells and their associated seals:

1. To determine if fluid compartments and their associated pressure seals showed unique organic geochemical fingerprints that might help in their future detection, particularly in shales where the repeat formation tester (RFT), currently the most reliable means of obtaining accurate downhole pressures (Hunt, 1990), gives no data. The problem arises because the RFT operates by punching a hole into the adjacent sedimentary rock in the well, collecting about one-half cup of water, and measuring its pressure. Because shales, for all practical purposes, extrude no water over the time period of the RFT measurement, the RFT is not useful for measuring shale pressures.
2. To gain preliminary information on the effects of pressure compartments and their associated seals on oil and gas distributions in sedimentary rocks.
3. To carry out preliminary research on how organic maturation and migration processes might contribute to pressuring and sealing mechanisms (versus occurring in parallel to independent inorganic sealing processes caused by the same time-temperature regime).

SAMPLES

Samples from two different geographic areas were examined in this work: drill cuttings samples from the Mix M J well (API 17-077-20241; lat. 30.67753; long. 91.47746) and Bizette R2 well (API 17-077-20290; lat. 30.67170; long. 91.51810) from the Moore-Sams field in the Louisiana Gulf Coast Tuscaloosa trend as described in Weedman et al. (1992) (Figure 1A), and from the Weaver No. 1 well in the N.W. Lindsay field of McClain County, Oklahoma of the Anadarko basin (Figure 1B, API No. 35-087-35445-00, location Section 17, T5N, R4W) as described in Tigert and Al-Shaieb (1990).

Samples from the two Gulf Coast wells represent intervals above, within, and below pressure transition zones as defined by RFT measurements (Weedman et al., 1992). The RFT is a downhole tool that operates by measuring the pressure in fluids extracted from sandstone intervals. In the case of the Mix well, water pressures of 8726 and 12,128 psi (60 and 84 MPa) were measured at the top and bottom of the pressure transition zone at depths of 18,586 ft (5665 m) and 18,881 ft (5755 m), respectively. The pressure gradients at the bottom and top of the same zone were 0.469 and 0.649 psi/ft (10.4 and 14.4 kPa/m, respectively) compared to a normal hydrostatic gradient of 0.43 to 0.53 psi/ft (9.54 to 11.8 kPa/m, depending on the salinity of the pore waters). For the Bizette-2 well pressure transition zone, pressures of 8700 and 11,759 psi (60.0 and 79.5 MPa) and gradients 0.469 and 0.649 psi/ft (10.4 and 14.4 kPa/m) were measured at depths of 18,445 ft (5622 m) and 18,734 ft (5710 m), respectively.

Only cuttings were available from the pressure transition zones of Mix and Bizette 2 wells. Because of potential problems with downhole slumping and drilling contamination, these were examined carefully using organic petrographic microscopy to ensure that drilling contamination was minimal. There was no mention of drilling additives in the drilling reports.

Data are also presented for conventional cores from the Weaver well of the Oklahoma Anadarko basin (Figure 1B) (Tigert and Al-Shaieb, 1990), which penetrates a much weaker pressure transition zone than the one described above for the Gulf Coast. In this zone, a transition from underpressured to slightly overpressured conditions, as defined regionally by final shut-in pressure from drill-stem test (DST) measurements, was found in the depth range of 11,000 to 12,000 ft (3353 to 3658 m). However, the highest average gradient measured in the overpressured zone was only about 0.51 psi/ft (11.3 kPa/m) at the bottom of the pressure transition zone, or seal zone.

METHODS

Pyrolysis, pyrolysis gas chromatography (Py-GC), and pyrolysis gas chromatography mass spectroscopy

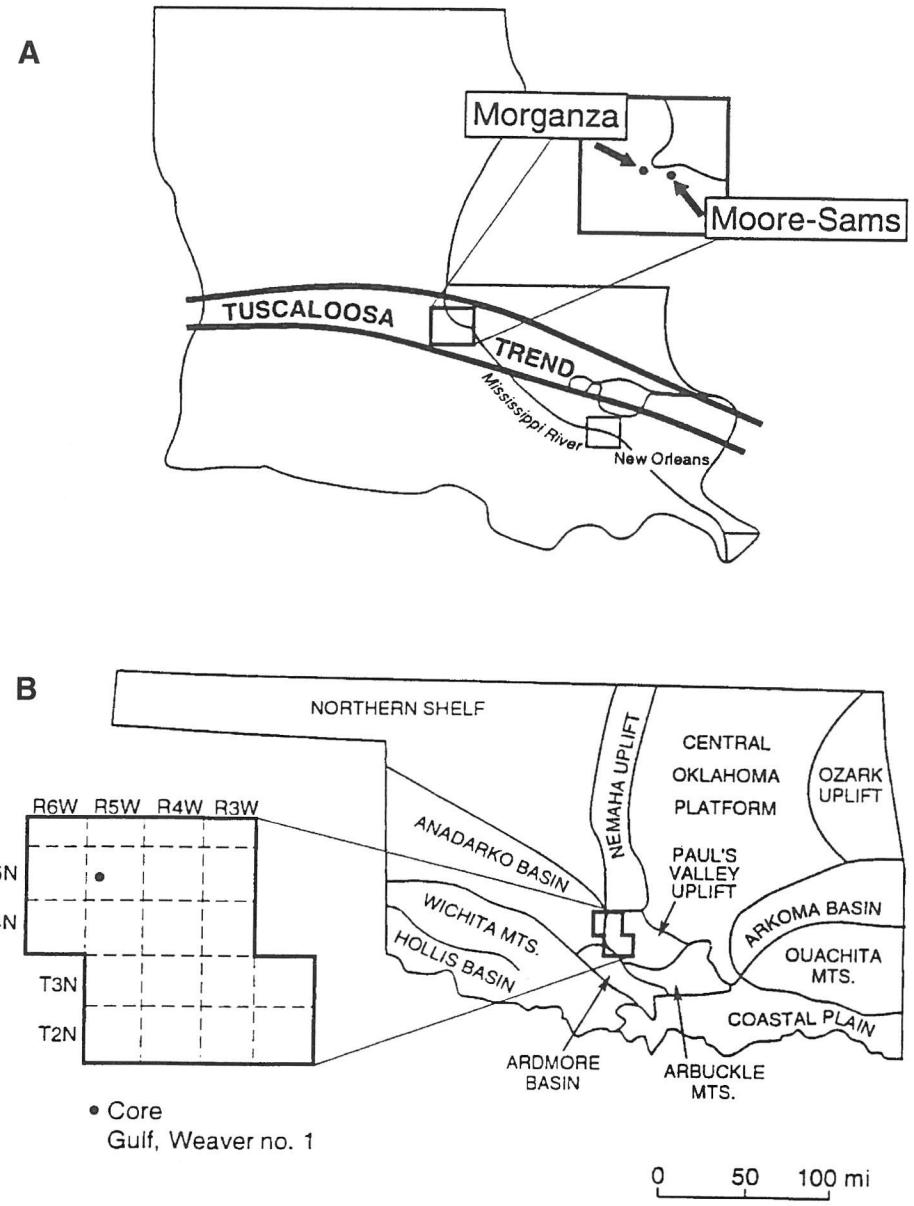

Figure 1. Location of (A) Mix and Bizette wells, Louisiana Gulf Coast Tuscaloosa Trend and (B) Weaver well, Anadarko basin, Oklahoma.

(Py-GCMS) were performed with a Chemical Data Systems (CDS) Pyroprobe used in the desorption mode as described previously (Whelan et al., 1990; Tarafa et al., 1988). The procedures and data are similar, but not identical to, those obtained from Rock Eval pyrolysis (Espitalié et al., 1984; Espitalié, 1986). Typically, a 10 to 50 mg sample of either whole rock or kerogen is heated at a constant rate of 30°C/min in a helium flow. The total volatilized hydrocarbons that evolve as a function of temperature are measured with a flame ionization detector to produce a pyrogram, such as those in Figure 3, where P_1 represents the volatile lower molecular weight constituents ($<C_{25}$) of generated petroleum and P_2 represents the sum of the residual petroleum generating capacity of the sedimentary rock. P_2 is derived from the sum of the heavier, less volatile ($>C_{25}$) cracking of more polar constituents of the in situ generated petroleum and petroleum generated by pyrolytic cracking of kerogen (Tarafa et al., 1988 and references cited). Cracking products of asphaltenes (the most polar component of petroleum) often elute along with the less volatile oil components as a low temperature shoulder on the front of the P_2 peak (Tarafa et al., 1988).

T_{max} is the temperature at which maximum P_2 evolution occurs. If P_2 is only a product of kerogen cracking with no contribution from residual or migrated heavy oil or asphaltene cracking, T_{max} generally increases with the thermal maturity, or time-temperature history, of the kerogen in the sedimentary rock (Espitalié, 1986; Peters, 1986). The T_{max} values reported here are the actual temperatures of the sample measured by a thermocouple placed adjacent to the sample. These are typically 50 to 60°C higher than values obtained from the Rock Eval pyrolysis instrument (Espitalié et al., 1977, 1984; Whelan et al., 1986).

The production index (P.I.) is the ratio of P_1 to the sum of P_1 plus P_2 and represents the ratio of the $<C_{25}$

fraction of generated in situ petroleum to total generation potential. In this paper, the low and high temperature pyrolysis peaks are referred to as P_1 and P_2, respectively, rather than S_1 and S_2 as used for Rock Eval pyrolysis, because of the differences in separation characteristics, responses, and T_{max} temperatures in the CDS Pyroprobe and Rock Eval pyrolysis instruments.

Total carbon and total organic carbon (TOC) measurements were performed using a Coulemetrics CO_2 Coulometer by procedures previously described (Whelan et al., 1990).

Iatroscan analysis was performed on an Iatroscan TH-10, Mk IV (Iatron Labs, Inc., Tokyo), equipped with a flame ionization detector (FID), interfaced with an electronic integrator (Perkin-Elmer LCI-100) by the method of Karlsen and Larter (1991).

Vitrinite determinations were made on whole rock cuttings samples that were coarsely ground to a particle size of approximately 2 mm and cold set in an epoxy resin. The samples were then ground and polished according to standard procedure (ICCP, 1963, 1971, 1975). Vitrinite determinations were performed on a Zeiss Universal microscope-photometer system. The system and determinations were standardized according to Stach et al. (1982). Determinations represent the mean reflectance population of indigenous, randomly oriented vitrinite particles (% R_o average), i.e., not those deemed as reworked from older sediments or sedimentary rocks. Fluorescence blue-light examination was performed on the same microscope fitted with a 100w HBO mercury arc bulb and using an LP520, BP450-490 filter set.

The term *matrix bitumen stain* refers to bitumen that impregnates the mineral matrix, does not readily polish, and often exhibits weak dark-brown fluorescence in blue light. Solid bitumen is that portion of the bitumen which takes a polish and can be identified in incident white light and fluorescence light (Jacob, 1989). These terms are distinct from matrix bituminite as characterized by Creaney (1980), which refers to very finely dispersed indistinguishable amorphous material within the mineral matrix and is analogous to the amorphous and perhaps some fraction of the liptodetrinitic material referred to in kerogen concentrates.

RESULTS

Summary of Observations from the Bizette 2 and Mix Wells, Louisiana Gulf Coast

Pyrolysis Data, Mix Well

Pyrolysis was carried out on samples from within as well as above and below the pressure seal zone, as defined by the pressure transition zone. P_1, P_2, TC, TOC, P_1/TOC, P_2/TOC, P.I., and T_{max} are given in Table 1, and downhole profiles are plotted in Figure 2. The solid horizontal lines show the pressure transition or pressure seal zone, as defined by the RFT measurements. Distinct changes in all pyrolysis parameters can be observed just above as well as within and below the pressure seal zone in comparison to shallower and deeper intervals. P_1, P_1/TOC, and P.I. maximize at the top and just under the seal for the Mix well (Figure 2) reflecting a maxima in light ($<C_{25}$) generated petroleum in this zone. A gradual decrease in both P_1 and P.I. is also observed with increasing depth in the seal zone. Based on P.I. values, all of the Mix samples are influenced by either generated or migrated petroleum hydrocarbons: P.I. values of less than 0.1 are typical of immature or organic lean intervals; 0.1 to 0.4 is typical of source rocks within the oil generation window; values of 0.4 to 1 are typical of sedimentary rocks containing migrated hydrocarbons (Peters, 1986; Vandenbroucke and Durand, 1983; Whelan et al., 1986). P_2 shows an increase approaching the top of the pressure seal zone and remains fairly high through the pressure transition zone and just below.

The lithology and shapes of the P_1 and P_2 peaks as a function of depth for the Mix well are shown in Figure 3. The low temperature shoulder, indicative of asphaltene and C_{25+} components of generated oil (Clementz, 1979; Tarafa et al., 1988), is commonly observed on the front of P_2 peak (e.g., indicated by circles for 17,690 and 18,570 ft [5392 and 5660 m] samples in Figure 3). This low-temperature P_2 shoulder is present in most of the Mix well samples shown in Figure 3, including those above and below as well as within the seal zone. An enhancement of the area of the shoulder in relation to the rest of the pyrogram is most evident through and below the seal zone.

T_{max} shows an overall decrease with depth in the Mix well (Figure 2F), contrary to the more normal case where T_{max} increases with increasing depth and maturity. This decreasing T_{max} trend is particularly pronounced within the seal zone and is due to the presence of heavy and polar components of generated or migrated petroleum within this zone (discussed below). T_{max} values start at 490°C at the top of the seal zone and decrease to 480°C at the bottom (equivalent to a decrease from 440 to 430°C on the Rock Eval pyrolysis T_{max} scale) and below the seal (Figure 2F and Table 1).

The partial hydrocarbon compositions of P_1 for the Mix well samples for the samples numbered 7, 11, 14, 17, and 21 (Table 1 and Figure 2A) are shown in Figure 4. Only the lighter hydrocarbon compositions are shown because they are the most diagnostic of various migration processes (Thompson, 1979, 1988; Leythaeuser et al., 1980; Hunt, 1985; Whelan et al., 1984). Mix #7, just above the seal zone at 18,580 ft (5663 m), shows a predominance of the aromatic hydrocarbon xylene, a hydrocarbon that tends to migrate easily with the aqueous phase (Thompson, 1979, 1988; Whelan et al., 1984). Samples crossing from the top to the bottom of the seal zone, Mix #11 (18,700 ft, 5700 m), Mix #14 (18,790 ft, 5727 m), and Mix #17 (18,880 ft, 5756 m), show a general progression from a predominance of the lowest molecular weight alkane (nC_8) toward the heavier nC_{14} at the bottom of the seal in Mix #17. In contrast, Mix #21 at 19,000 ft (5791 m), just below the seal, shows no

Table 1. Summary of pyrolysis, TC, TOC, and vitrinite reflectance results, Mix, Bizette, and Weaver wells.

Depth (ft)	Sample no.	P_1 (mg HC/g rock)	P_2 (mg HC/g rock)	P.I.*	T_{max} (°C) (CDS)	T_{max} Rock Eval calculated**	TC (%)	TOC (%)	P_1/TOC (mg HC/g TOC)	P_2/TOC (mg HC/g TOC)	Iatroscan yields (Polar fraction) (mg/g rock)	% R_o#	Number of points
Mix Well													
17,440													
17,470	1	4.29	7.71	0.36	492	442	3.93	1.9	226	406		0.84±0.11	11
17,660													
17,690	2	0.07	0.38	0.15	508	458	1	0.43	16	89		0.97±0.10	12
18,060													
18,090	3	0.35	0.74	0.32	489	439	1.05	1.06	33	70		0.94±0.10	6
18,150													
18,180	4	0.20	1.33	0.13	488	438	1.69	1.2	17	111		0.94±0.02	5
18,430													
18,450	5	0.65	3.09	0.17	488	438	2.97	1.61	40	192		0.93±0.04	4
18,560													
18,570	6	3.19	4.30	0.43	495	445	2.62	2.29	139	188	2.71	0.93±0.08	6
18,580	7	2.69	3.08	0.47	490	440	1.71	0.83	324	371		0.91±0.09	8
18,610	8	6.93	5.16	0.57	492	442	2.11	1.21	572	426		0.90±0.09	4
18,640	9	3.62	3.63	0.50	490	440	2.53	1.76	206	206		1.05±0.09	12
18,670	10	6.79	6.51	0.51	490	440	2.38	1.3	522	500	3.6	1.20±0.08	6
18,700	11	2.98	3.39	0.47	483	433	2.6	1.63	183	203			
18,730	12	2.65	6.10	0.30	498	448	2.41	1.7	156	359		1.29±0.09	24
18,760	13	2.85	3.43	0.45	482	432	2.15	1.61	177	213	5.17	1.29±0.06	12
18,790	14	3.33	3.86	0.46	481	431	2.67	1.59	210	242		1.24±0.08	5
18,820	15	4.09	5.51	0.43	479	429	2.61	1.58	259	349		1.28±0.09	18
18,850	16	2.90	4.38	0.40	478	428	2.35	1.59	183	276		1.29±0.08	9
18,880	17	2.24	4.57	0.33	488	438	1.73	1.27	176	360			
18,900	18	1.68	4.08	0.29	482	432	2.82	2.02	83	202	10.3	1.26±0.10	5
18,930	19	1.77	1.36	0.57	481	431	1.74	0.95	187	144		1.23±0.11	7
18,960	20	3.82	4.83	0.44	486	436	1.93	1.33	287	363	5.26		
19,000	21	5.13	5.59	0.48	478	428	2.78	1.95	263	286		1.31±0.07	4
19,010	22	2.56	1.16	0.69	488	438	1.56	1.25	205	93			
Bizette Well													
17,775	1	0.05	0.32	0.12	522	472	1.12	0.74	6.1	44		1.08±0.09	10
17,875	2	0.06	0.36	0.14	562	512	1.35	0.81	7.0	45			
18,025	3	0.07	0.37	0.16	523	473	2.31	0.89	8.2	42			
18,150	4	0.07	0.85	0.078	510	460	2.56	2.15	3.3	39			
18,300	5	0.14	0.46	0.24	528	478	1.22	0.93	15.4	4.9			

* P.I. = $P_1/(P_1 + P_2)$.

** Calculated Rock Eval T_{max} = CDS T_{max} – 50°C.

\# Average vitrinite reflectance % in oil (ne1.517@23°C) @ 546 nm.

Underlined values designate values within the pressure transition zone.

Continued on next page

Table 1. Summary of pyrolysis, TC, TOC, and vitrinite reflectance results, Mix, Bizette, and Weaver wells (continued).

Depth (ft)	Sample no.	P_1 (mg HC/g rock)	P_2 (mg HC/g rock)	P.I.*	T_{max} (°C) (CDS)	T_{max} Rock Eval calculated**	TC (%)	TOC (%)	P_1/TOC (mg HC/g TOC)	P_2/TOC (mg HC/g TOC)	Iatroscan yields (Polar fraction) (mg/g rock)	% R_o#	Number of points
18,325											8.83		
18,350	7	0.14	0.44	0.24	507	457	2.18	1.21	11	36			
18,412	8	0.01	0.96	0.006	441	391	2.45	1.19	0.53	81			
18,450	9	0.62	2.88	0.18	487	437	4.44	4.32	14	67		0.90±0.09	12
18,475	10	0.73	0.86	0.46	477	427	1.93	1.93	38	45		0.98±0.08	15
18,500	11	0.61	0.61	0.50	559	509	1.74	1.92	32	32	20.04	1.10±0.07	20
18,525	12	6.88	6.52	0.51	495	445	3.09	3.5	197	186	25.2	1.02±0.09	20
18,550	13	3.01	3.97	0.43	502	452	2.63	2.44	123	163	4.36		
18,575	14	7.91	8.50	0.48	489	439	3.71	3.4	233	250			
18,625	15	13.47	5.42	0.71	482	432	4.46	4.1	329	132	6.78		
18,650	16	1.40	3.04	0.31	491	441	2.57	2.54	55	120			
18,675	17	4.16	6.43	0.39	504	454	3.64	3.1	134	207			
Weaver Well													
10,190	1	0.0031	0.136	0.02	504	454	0.14	0.14	2.21	97			
10,537	2	0.0012	0.07	0.02	490	440	8.05	0.25	0.48	28		0.50±0.09	4
11,014	3	0.014	0.181	0.07	514	464	1.14	0.13	10.8	139		0.46±0.02	4
11,057	4	0.0064	0.0978	0.06	512	462	0.24	0.08	8.00	122			
11,085	5	0.0028	0.151	0.02	495	445	0.08	0.08	3.50	189		0.97±0.05	4
11,171	6	0.0052	0.114	0.04	488	438	1.83	0.18	2.89	63		0.75±0.09	6
11,204	7	0.016	0.758	0.02	504	454	0.84	0.63	3	120		0.60±0.10	10
11,274	8	0.013	0.654	0.02	507	457	1.68	0.53	2.45	123		0.82±0.02	4
11,344	9	0.294	1.033	0.22	519	469	0.4	0.36	82	287		0.90±0.06	8
11,384	10	0.0011	0.08	0.01	500	450	0.27	0.15	1	53		0.86±0.05	10
11,446	11	0.01	0.333	0.03	498	448	0.62	0.33	3.03	101		0.95±0.06	20
11,472	12	0.002	0.087	0.02	495	445	0.17	0.1	2.00	87			
11,521	13	0.0016	0.157	0.01	500	450	4.85	0.3	0.53	52			
11,543	14	0.0025	0.143	0.02	495	445	1.55	0.18	1.39	79			
11,556	15	0.003	0.464	0.01	498	448	2.47	0.43	0.70	108			
11,650	16	0.0044	0.318	0.01	488	438	0.46	0.43	1.02	74		0.89±0.05	4
11,720	17	0.0068	0.146	0.04	493	443	0.43	0.3	2.27	49			
11,961	18	0.017	0.229	0.07	502	452	3.22	0.43	3.95	53		1.02±0.04	8
11,992	19	0.003	0.059	0.05	486	436	0.4	0.14	2.14	42			
12,068	20	0.016	0.08	0.17	492	442	8.42	0.66	2.42	12			

Continued on next page

* P.I. = $P_1/(P_1 + P_2)$.

** Calculated Rock Eval T_{max} = CDS T_{max} – 50°C.

\# Average vitrinite reflectance % in oil (ne1.517@23°C) @ 546 nm.

Underlined values designate values within the pressure transition zone.

Table 1. (Continued)

Source Rock Classification (from Peters, 1986)
Typical values of the parameters above:

Source rock quality	P_1 (mg HC/g rock)	P_2 (mg HC/g rock)	TOC (%)
Poor	0 to 0.5	0 to 2.5	0 to 0.5
Fair	0.5 to 1	2.5 to 5	0.5 to 1
Good	1 to 2	5 to 10	1 to 2
Very good	2 plus	10 plus	2 plus

Typical source rock maturation values (from Tissot and Welte, 1984; Peters, 1986; Mukhopadhyay, 1992)

	P.I.*	T_{max} Rock Eval	$\%R_o$ # (Kerogen Type II/III)
Immature		<435	<0.45%
Marginally mature	~0.1	435 to 445	~0.45–0.5%
Total oil window			0.55–1.1%
Maximum oil generation zone	~0.1 to 0.4	435 to 470	~0.7–0.9%
Wet gas zone			~1.1–2%
Dry gas zone		>470	>2.0%

* P.I. = $P_1/(P_1 + P_2)$.
** Calculated Rock Eval T_{max} = CDS T_{max} – 50°C.
\# Average vitrinite reflectance % in oil (ne1.517@23°C) @ 546 nm.

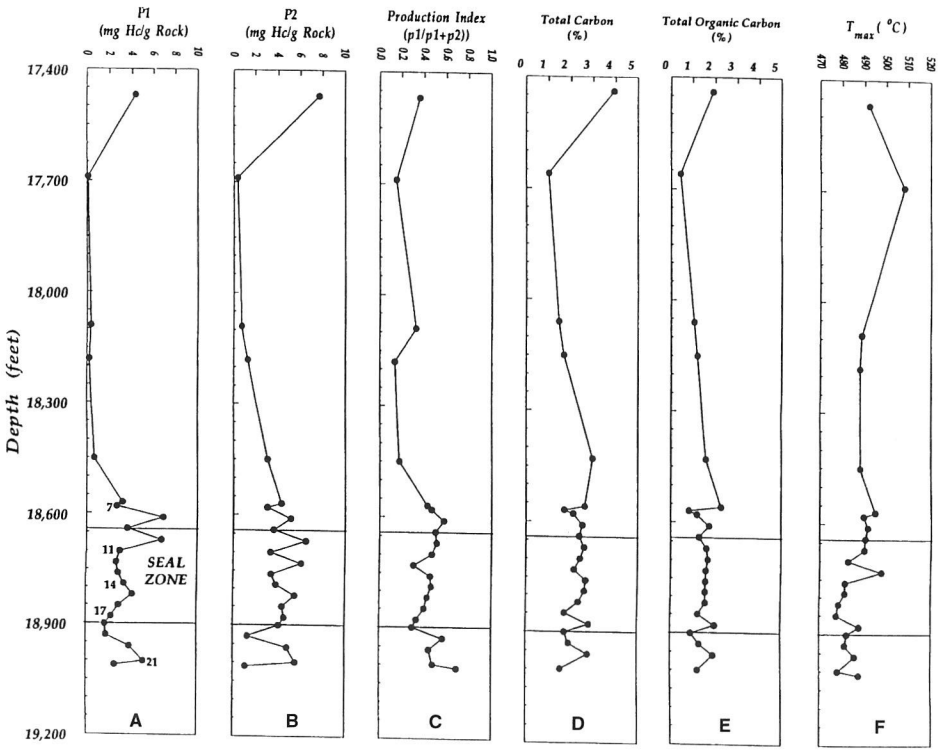

Figure 2. Pyrolysis data across pressure seal, Mix well—Gulf Coast Tuscaloosa trend.

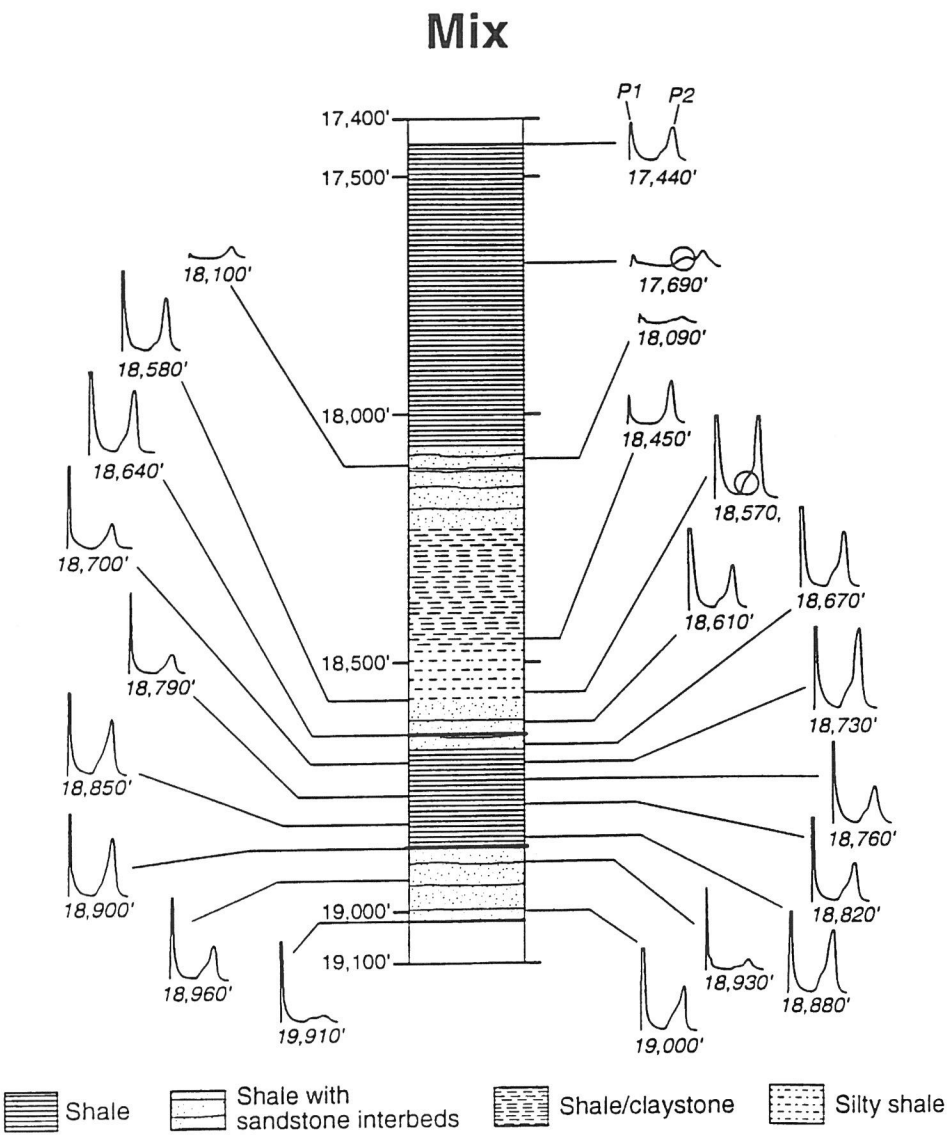

Figure 3. Downhole pyrograms, Mix well. Pressure seal is located between the heavy lines.

particular predominant alkane—all of the nC_7 through nC_{14} hydrocarbons, including the aromatic compounds toluene and xylene, are present.

Unlike the P_1 products, the compositions of P_2 products (Figure 5) are similar, except for depletion of the heavier hydrocarbons nC_{14} and nC_{16} in Mix #14 and Mix #17. The similarity in P_2 products is consistent with the initial cracking of a high molecular weight organic matrix (i.e., asphaltene or kerogen), which is similar for all of the Mix samples (Larter, 1984; Whelan et al., 1980, 1986; Dembicki et al., 1983; Horsfield, 1984).

Pyrolysis Data, Bizette Well

Downhole profiles of TOC and pyrolysis data are shown in Table 1. TOC is 0.7 to 1.2% above the pressure seal zone and increases across and below the seal zone with a maximum value of 4.3% at the top of the seal (18,450 ft, 5624 m). Increases are apparent for P_1, P_2, P_1/TOC, P_2/TOC, and P.I. at the bottom and beneath the seal. P_2 and P_2/TOC also show maxima at the top of the seal zone. P.I. increases to values above 0.4 within and below the seal, probably due to petroleum that has migrated into this silty and sandy shale (Figure 6).

The difference between the generally low amounts of petroleum above the seal and the much larger amounts just above, within, and below is striking in the downhole pyrograms (Figure 6). Increasing light oil (strong P_1) as well as polar and/or heavy oil constituents (shoulder on the front of the P_2 peak) throughout deeper intervals of the Bizette well can be observed in the downhole pyrograms (Figure 6).

The C_7 to C_{16} hydrocarbon compositions of P_1 and P_2 for several Bizette samples from above, below, and within the seal zone were also examined for this well. Unfortunately, sample coverage is not extensive enough to discern whether or not the hydrocarbon patterns observed previously in the Mix well also apply here.

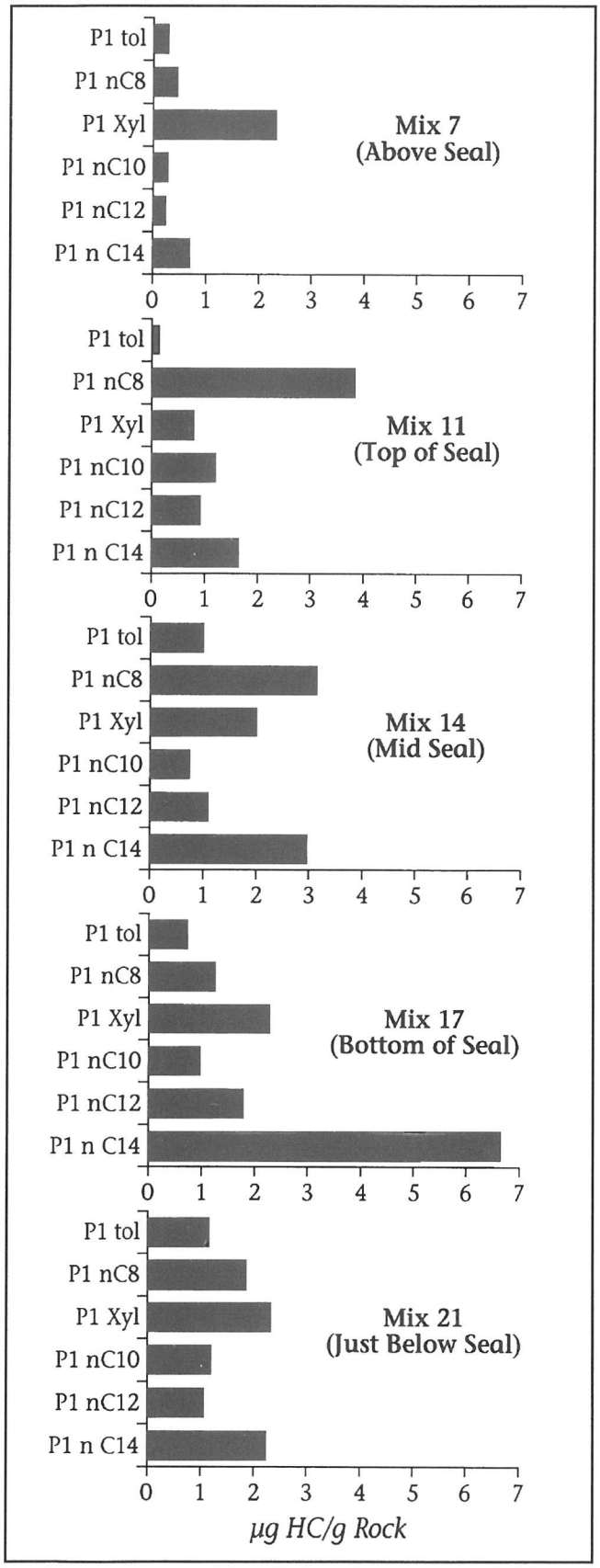

Figure 4. Composition of C_7 to C_{14} hydrocarbons in P_1, Mix well.

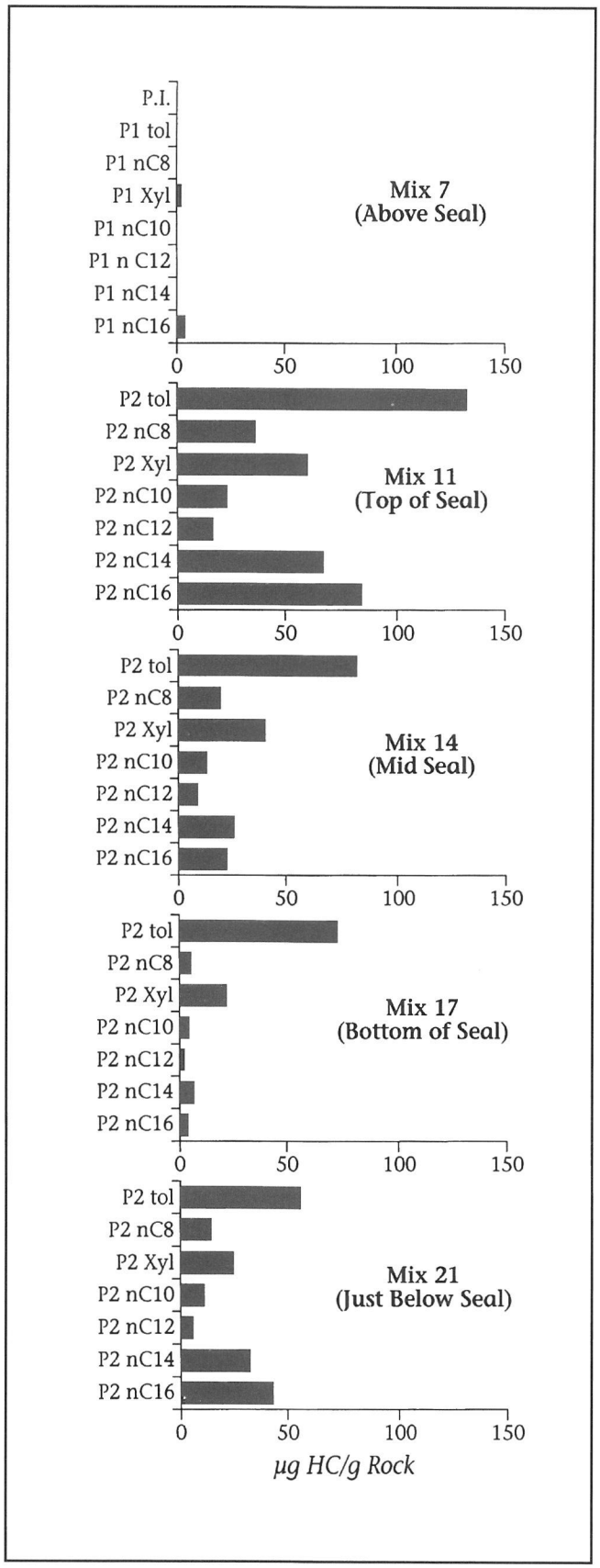

Figure 5. Composition of C_7 to C_{14} hydrocarbons in P_2, Mix well.

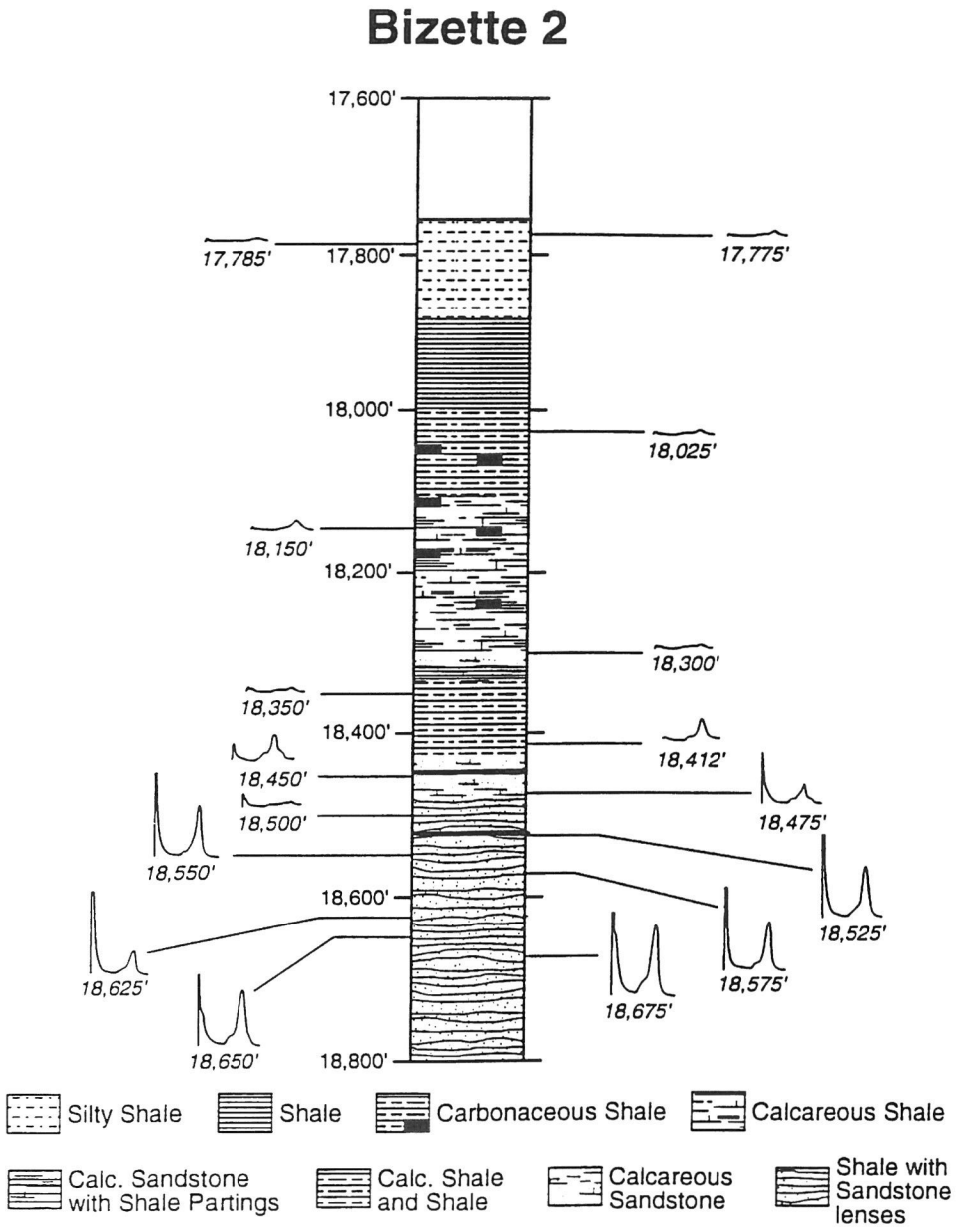

Figure 6. Downhole pyrograms, Bizette 2 well—Gulf Coast Tuscaloosa trend. Pressure seal is located between the heavy lines.

Microscope Observations

Mix Well

Sample Description

Eighteen drill cuttings samples between 17,445 and 19,000 ft (5317 and 5791 m) were prepared for thermal maturation determinations by vitrinite reflectance and for simultaneous petrographic observation. Samples above, within, and below the seal show an intimate association of quartz, carbonate, pyrite, bitumen, asphaltenes, and micrinite (a granular, <1 mm residual product from hydrocarbon generation from bituminite).

The sampled section spans a depth interval of 1560 ft (475 m). The section begins in Cretaceous sedimentary rocks at the top of the upper Tuscaloosa Formation (17,440 ft, 5317 m), as defined by the Bain marker bed from gamma-ray and resistivity logs (Weedman et al. 1992). Repeat formation tester measurements (RFT, trademark of Schlumberger and described in detail in Weedman et al., 1992) show an increase from normally pressured to overpressured strata within the Lower Tuscaloosa Formation as shown in Figure 7 along with the well log data. This pressure transition zone between 18,649 and 18,910 ft (5684 and 5764 m) is interpreted in this paper as a zone containing a permeability barrier to escaping overpressured fluids. This barrier is referred to as a pressure seal.

Within the Upper Tuscaloosa Formation, two microlithotypes are characterized as interbedded thin laminated shales (≈0.5–1.0% TOC) and silty shales (≈<0.5% TOC). Both microlithologies contain terrestri-

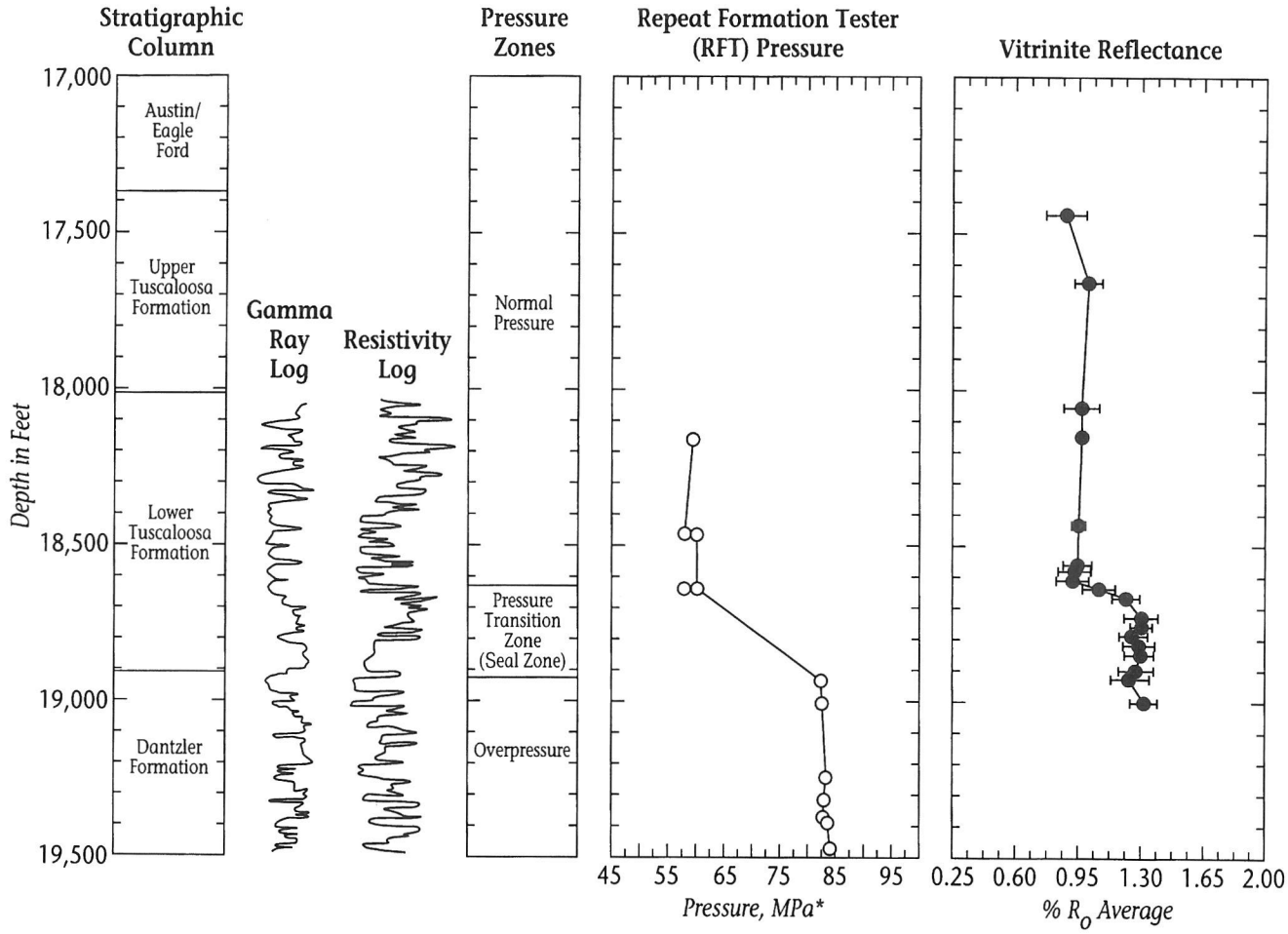

Figure 7. Vitrinite reflectance trend across pressure seal, Gulf Coast Mix well. Typical vitrinite reflectance values for the peak oil generation zone are 0.8 to 1.2%; those for the gas generation window are typically 1.1 to 1.8%. Also shown are pressure and well log data (gamma-ray and resistivity logs).

ally derived organic matter characterized as Type III/IV kerogen (Tissot and Welte, 1984; Mukhopadhyay and Wade, 1990).

Fifteen samples from the lower Tuscaloosa Formation were analyzed spanning a depth interval from 18,060 to 18,930 ft (5505 to 5770 m). These are characterized by interbedded silty shales, siltstones, and laminated organic-rich shales (≈1–2% TOC). This shale is rich in matrix bitumen staining and framboidal pyrite and shows an increase in fine rutile (TiO_2) needles in the mineral matrix with depth. Quartz grains in the silty shales are generally dispersed but occasionally form more tightly packed domains. The organic material in the shales is dominated by terrestrially derived Type III and III/IV solid organic particles. A sandstone at 18,150 ft (5532 m) contains high abundance of dark brown matrix bitumen surrounding subrounded quartz grains. This bitumen fluoresces dark orange-brown in blue light.

Between 18,580 and 18,640 ft (5663 and 5681 m), a well-laminated shale containing high abundances of terrestrially derived Type III organic material (≈2.5% TOC) is interbedded with a lean (≈<0.5% TOC) silty shale containing well-rounded quartz grains that are probably dissociated foraminifera chambers. This shale is heavily stained with dark-brown matrix bitumen and contains abundant fine grains of pyrite evenly dispersed throughout the matrix. The cuttings sample below 18,610 ft (5672 m) is dominated by a fine-grained sandstone. Pyrite infills pit on the surface of many subangular quartz grains. There is an enrichment of coarser phyllosilicate laths of rutile in the matrix of some silty shale cuttings at this depth. Acicular radiating groups (rutile) occur in the interior of quartz grains but are more abundant in the shaly matrix where multiple knee-shaped twins occasionally form wheels. This may be indicative of an igneous source of the grains, although it may be representative of low-grade metamorphism. Between 18,670 and 18,790 ft (5691 and 5727 m), there is little variation in organic facies from predominantly terrestrial Type III woody material. The microlithologies show a similar distribution of laminated shales, silty shales, and fine sandstones. In different cuttings of the silty shale the quartz grain shapes range from subangular to subrounded and in general these grains are poorly sorted

and are persistently matrix supported, although a minor siltstone lithology at 18,670 ft (5691 m) contains tightly packed elongated grains (grain supported). Cracks are apparent in the larger quartz grains at 18,730 ft (5709 m) and in a siltstone at 18,760 ft (5718 m) where they are surrounded by smaller quartz grains that are stained with light-brown bitumen that fluoresces a dull orange-brown in blue light.

Three samples between 18,820 and 18,900 ft (5736 and 5761 m) contain cuttings of an unusual coarse-grained silty shale in which the matrix minerals exhibit a very heavy dark-brown–black nonfluorescing bitumen stain. The quartz grains associated with this lithology are cracked. It is difficult to assess whether these cracks are a feature of pressure solution at grain contacts due to the limited information available from a two-dimensional viewing plane. An important microlithologic observation noted from this sample is the presence of cuttings of a tightly packed siltstone in which quartz grains are elongate. This grain packing produces very fine sutures at grain margins that yield an extremely low porosity and could conceivably be considered as a permeability barrier. Although the extent of this lithology is difficult to determine from cuttings samples alone, it may be represented by a finger-shaped drop in the gamma-ray log at ~18,000 ft (5486 m) (Figure 7). An increase in matrix bitumen staining occurs at 18,850 ft (5745 m), and by 18,900 ft (5761 m) there is an abundance of disseminated fine pyrite, micrinite, and heavy bitumen staining of the shaly mineral ground mass.

A poorly laminated shale containing a low to moderate (≈0.5–1% TOC) abundance of terrestrial Type III and Type III/IV organic matter occurs at 18,930 ft (5770 m). There is only a faint matrix bitumen staining in this microlithology. A second microlithology consists of a silty shale that contains subangular grains of quartz dispersed in a shaly matrix. These quartz grains are not cracked.

One sample collected from the Dantzler Formation (19,000 ft, 5791 m) contains a tightly packed silty shale in which the matrix minerals are heavily stained with dark-brown–black bitumen. Small quartz grains (≈10 μm ϕ) also appear to be cracked, but it is impossible to determine, using incident light techniques, whether these cracks have been formed by pressure solution or are due to the provenance of the sedimentary rocks. The organic facies remains terrestrial Type III in this sample.

Thermal Maturity

Figure 7 shows a vitrinite reflectance depth plot for the Mix well and data are shown in Table 1. Vitrinite reflectance values remain fairly constant between 17,440 and 18,640 ft (5317 and 5681 m) at about 0.94% R_o. A maturation jump to 1.20% R_o occurs at 18,730 ft (5709 m). This jump is coincidental with an initial increase in formation pressures at the top of a pressure transition zone as shown in Figure 7. The maturity remains constant at about 1.28% R_o throughout this zone. These maturity determinations together with the organic matter type are consistent with a capacity for the generation of gaseous hydrocarbons.

Summary

The organic facies remains virtually constant throughout the depth interval and can be characterized as terrestrial-derived organic material comprised of woody Type III kerogen and inertinitic Type IV kerogen with a capacity at this thermal maturity for gas generation. The sudden occurrence of rutile and peculiarly cracked quartz surrounded by heavy bitumen staining is coincidental with the pressure transition zone. This observation seems to be consistent with those reported in Weedman et al. (1992) where they describe unusually fractured quartz grains in a quartz-rich matrix with closely spaced pressure-solution seams that are seen only within the pressure transition zone. Further work is in progress to determine if these fractures might be caused by the overpressuring or whether they are an artifact of drilling. In any case, the present work suggests that these fractures, whatever their origin, are fairly characteristic of the pressure transition zone.

Bizette Well

Samples from this well showed lithologies and organic material (Type III/IV) similar to that observed in Mix (Figure 6). Reliable vitrinite data were more difficult to obtain because of the oxidation of the vitrinite. However, available data are shown in Table 1. Solid bitumen asphaltic material was present together with bitumen staining and framboidal pyrite above the seal in this well. Just above the seal, heavy organic staining, a micrinitic residue, indicative that oil generation has occurred, and quartz grains surrounded by calcite and pyrobitumen were present. Kerogen Type III persists into the middle and bottom of the seal, along with occurrences of pyrite, micrinite, secondary cementation, and etching of quartz grains. Asphalt that has passed through the oil window (termed here as pyrobitumen; Hunt, 1979) was evident as 25% of the organic matter in samples from 18,500 to 18,525 ft (5639 to 5646 m) at the bottom of the seal, giving an indication of the higher maturity in comparison to samples above the seal. Thermal maturity is in the range of 0.90 to 1.10% R_o, which is at the end of the oil window.

Iatroscan Results

Mix and Bizette Wells

Both organic petrographic and pyrolysis data showed the presence of asphaltic material in the vicinity of the seal zones. The approximate relative concentrations of this fraction were determined by Iatroscan (Table 1).

Relatively high amounts of asphaltenes are present in all four of the Mix samples examined, one from above, two from within, and one from below the seal. These results are in good agreement with microscopic and pyrolysis results described above which show the presence of asphaltenes as major organic phases in these intervals.

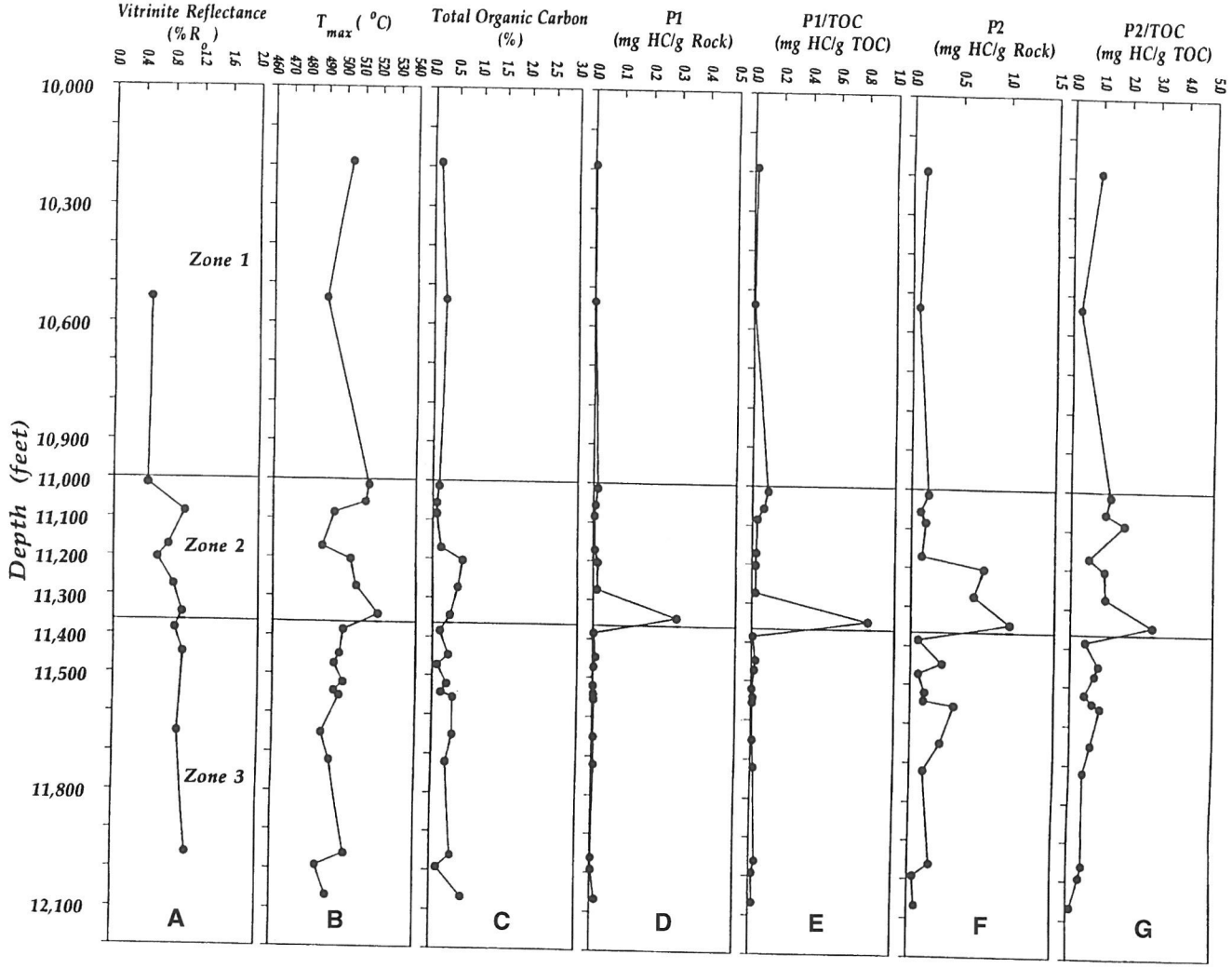

Figure 8. Vitrinite reflectance and pyrolysis data across pressure transition zone, Weaver well, Anadarko basin, Oklahoma.

Six samples from the Bizette well were also analyzed. High amounts of asphaltenes were detected within the seal zone, with lower amounts detected above and below.

Summary of Observations for Weaver Well, Anadarko Basin

Pyrolysis and petrographic microscopic studies were also carried out on much more organic lean core samples from the Weaver well, Anadarko basin, Oklahoma (Figure 1). The cores came from a much weaker pressure transition zone than that described above for the Gulf Coast wells. The downhole profiles of vitrinite reflectance and pyrolysis data (T_{max}, P_1, P_2, P_1/TOC, P_2/TOC, and P.I.) are shown in Table 1 and Figure 8, with zone 2 being the pressure transition zone and approximate position of the postulated upper seal (Tigert and Al-Shaieb, 1990). The values of TOC, P_1, P_2, and P.I. are all much lower than for Mix and Bizette. Several of these parameters show very erratic behavior, particularly within the pressure transition zone. All parameters related to P_1, P_2, or TOC show maxima within this interval.

Downhole vitrinite reflectances for Weaver are erratic because of changing organic facies and reworked particles. However, thermal maturity generally increases (from R_o 0.46 to 0.82%) through zone 2. These values cover the beginning to the middle of the oil window (see data from Peters, 1986, at the bottom of Table 1) over a relatively short depth interval of 400 ft. T_{max} goes through a minimum at ≈11,200 ft, as was also the case with the Mix well within the pressure transition zone, consistent with the presence of asphaltenes within the zone of maximum maturity within the seal zone. The vitrinite population examined at Weaver was more heterogeneous than was the case for the Mix well, so there is the possibility that the R_o changes were due to differences in organic matter type rather than maturation. The organic leanness coupled with the generally poorer quality of the vitrinite and the higher abundance of reworked phyto-

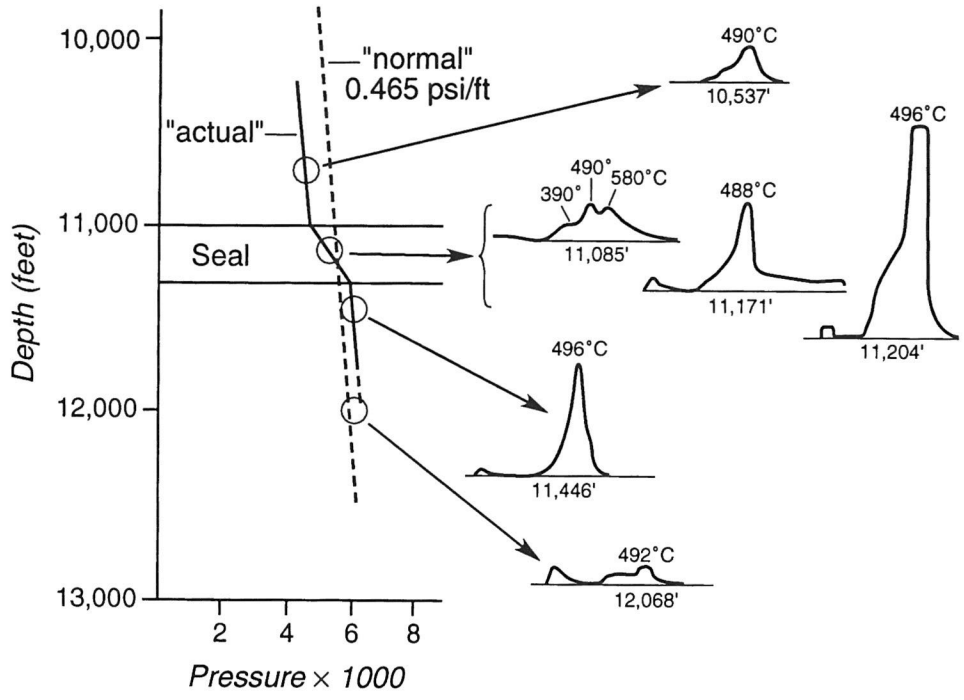

Figure 9. Representative pyrograms from across pressure transition zone, Weaver well, Anadarko basin, Oklahoma.

clasts have all affected the vitrinite measurements, producing greater scatter in the vitrinite determinations.

In spite of the much leaner nature of the Weaver samples, several pyrolysis parameters reflect zones containing asphaltene or heavy oil within the seal zone: the low values of T_{max} within the seal in zones of increasing R_o values (Figure 8) and the low-temperature lobe on many of the P_2 peaks (Figure 9). The lithology and organic petrography also show the close association between organic and inorganic phases, similar to those observed for the seal zones of Mix and Bizette wells. For example, in some intervals in the lower part of the pressure transition zone, pyrite that is heavily bitumen stained represents about 70% of the matrix mineral ground mass which surrounds carbonate grains and completely occupies the porosity in other clasts. At 11,204 ft (3415 m) in this well a fine sandstone contains rounded quartz grains that show an interesting inorganic and organic relationship. An organic bitumen directly coats the quartz grain margin that was encased by a subsequent phase of secondary silica overgrowths which trapped the bitumen next to the grain boundary. This relationship indicates hydrocarbons had entered these intervals prior to secondary cementation. These observations are similar to those made in deeper parts of the pressure seal in the Mix well.

Within the pressure transition zone (zone 2 in Figure 8), samples from 11,014 to 11,274 ft (3357 to 3436 m) are similar, have low to moderate organic contents (0.1 to 0.6% TOC), and have a shale lithology that becomes progressively more silty and calcite cemented with depth. There is also an increase in silicate dissolution at grain boundaries and precipitation of calcite as a cement with depth in fine sand to silty shale, but especially at 11,344 ft (3458 m). This sample contains considerable amounts of fine hydrocarbon wisps surrounding quartz grains in the calcite-cemented zones. Fine pyrite and matrix bitumen staining are closely associated and increase slightly in abundance with depth in this well. Pyrolysis P_1 and P.I. values are all low for this interval, however, increasing to somewhat higher values at the bottom of the pressure transition zone at 11,344 ft (3458 m). These changes occur within the zone showing some vitrinite reflectance change (Table 1 and Figure 8). Based on the microscopic and pyrolysis data, it seems probable that most of the relatively low amounts of TOC in zone 2 is present as heavy asphaltic bitumen.

Zone 3, below the pressure transition zone, is characterized as an organic lean interval from about 11,384 to 11,543 ft (3470 to 3519 m). Abundant fine pyrite is observed throughout this zone but is particularly abundant in samples from 11,446 to 11,650 ft (3489 to 3551 m). There is an increase in organic content by 11,720 ft (3572 m) that is dominated by pyrobitumen stringers closely associated with pyrite in a shaly claystone. Sedimentary rocks then become progressively more pyrobitumen dominated with depth to 11,921 ft (3634 m). This sample shows a moderate degree and constant intensity of bitumen staining and fine organic matter coatings of grains in a calcareous silty sand. In deeper intervals below 11,921 ft (3634 m), samples contain fine-grained calcite-cemented quartz sandstones but are organically lean with very low traces of matrix bitumen.

DISCUSSION

The most important observation that must be accommodated by any mechanism explaining the formation and maintenance of pressure seals over geo-

logic time is that the pressure seal zones must have extremely low permeability. Most estimations, including those of Iverson et al., this volume, show that only the most impermeable known rock types, such as unfractured metamorphic and igneous rocks or shales, even approach the required permeabilities. Therefore, it appears that some agent in addition to the rock must be contributing to these low permeabilities. We propose that sediment organic matter, particularly asphaltic materials and gas, are important components in forming such an impermeable pressure seal via the processes described below. We also propose that the observations about the nature of seals and the organic materials associated with them are giving important clues about the nature of the pressure sealing mechanism. These are discussed below.

1. Zoning of hydrocarbons has been observed within the pressure transition zone as discussed by Vandenbroucke and Durand (1983) for the Mahakam Delta and shown in Figure 4 for the Mix well. In both cases, lighter hydrocarbons tend to focus at the top of the seal, while heavier components predominate at the bottom of the seal. In addition, the GC patterns of the Mix P_2 pyrolysis products in comparison to P_1 show that migration phenomena, rather than changes in in situ organic source, are responsible for the P_1 C_8 to C_{14} hydrocarbon distributions. Within and below the seal, the P_2 GC patterns for all of the Mix samples are very similar. If the P_1 hydrocarbons were derived from a localized in situ source of kerogen or asphaltene, then the P_1 GC compositions should also be similar. In fact, the small changes in P_2 GC patterns are contrary to the P_1 patterns. Figure 5 shows enhancement of P_2 C_{14} and C_{16} products at the top of the seal (e.g., Mix 11) and some depletion at the bottom of the seal, just the opposite of the trends observed for the P_1 aliphatic hydrocarbon compositions (Figure 4). Therefore, migration processes must be invoked as the cause of the P_1 compositional gradients across the seal.

2. A sharp increase in thermal maturity gradient has been observed in pressure transition zones from the Gulf Coast Mix well (Figure 7). A weaker maturity increase also occurs for the Oklahoma Anadarko Weaver well (Figure 8) and possibly also in a Nova Scotia Sable Island Venture Field well (Well H-22 in Jansa and Norguera, 1990; Eglinton and Whelan, unpublished results). In addition, other microscopic differences between the two samples at the top and bottom of the Mix well seal zone are also consistent with a large maturity difference occurring over this very short depth interval. Thus, the 18,640 ft (5681 m) sample appears to contain bitumens typical of the oil window, while the sample at 18,850 ft (5745 m) shows higher maturity pyrobitumen, or bitumens that have passed through the oil window. In the Gulf Coast Bizette well, minimal fluorescence of organics is observed above the seal at 17,750 ft (5410 m), indicative of maturity around 0.9% R_o. However, at 18,425 ft (5616 m) and below, pyrobitumen is observed, diagnostic of higher maturities. Therefore, as with Mix, it appears that fairly large changes in maturity have occurred across the relatively short distance of seal zone. These maturational changes are accompanied by increasing amounts of carbonate cementation within and below the seal zone.

3. Precipitated asphalts and pyrobitumens are commonly an important part of the material in the pressure transition zone as shown by pyrolysis, petrographic microscopic results, and Iatroscan, as discussed above and shown in Figures 2 and 6 and in Table 1. This observation applies to the strong pressure transition zone in two Gulf Coast wells as well as to the much weaker pressure transition zone in Weaver well of the Anadarko basin, which has generally low TOC (Table 1). For example, one sample from the Weaver core (11,274 ft, 3436 m) shows extremely fine "sutures" infilled with bitumen giving the appearance of a grain coating or filling (Eglinton and Whelan, in preparation). Samples from Weaver differ from the Mix well in that their hydrocarbon phases are discontinuous. However, in all three wells, these organic precipitates are closely associated with secondary inorganic phases including carbonate cements and pyrite.

4. In both the Alaskan North Slope and in the Gulf Coast, some relatively low TOC rocks (1.5% TOC or less) appear to be producing and expelling oil (Huc and Hunt, 1980; Whelan et al., 1986), contrary to current wisdom that petroleum source rocks must contain enough TOC to form a separate oil phase before primary petroleum expulsion and migration can occur (Lewan, 1987; Cooles et al., 1986; Durand, 1988).

We propose that these observations can be explained as the consequence of: (1) the generation and migration of a separate gas phase in the deep subsurface; (2) the high solubility of oil in gas at high pressure; (3) the pressure dependence of the solubility of oil in gas; and (4) the low thermal conductivity of oil and gas.

Figure 10 shows an estimate of types and amounts of breakdown products of a typical Type III kerogen as it is heated with increasing burial along the gradient in

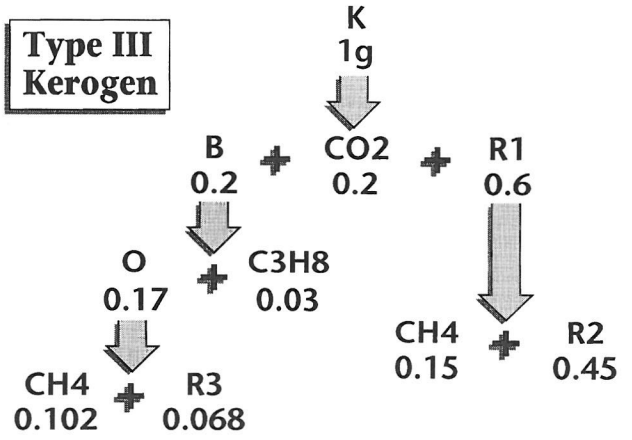

Figure 10. Initial estimation of breakdown of 1 g of Type III kerogen.

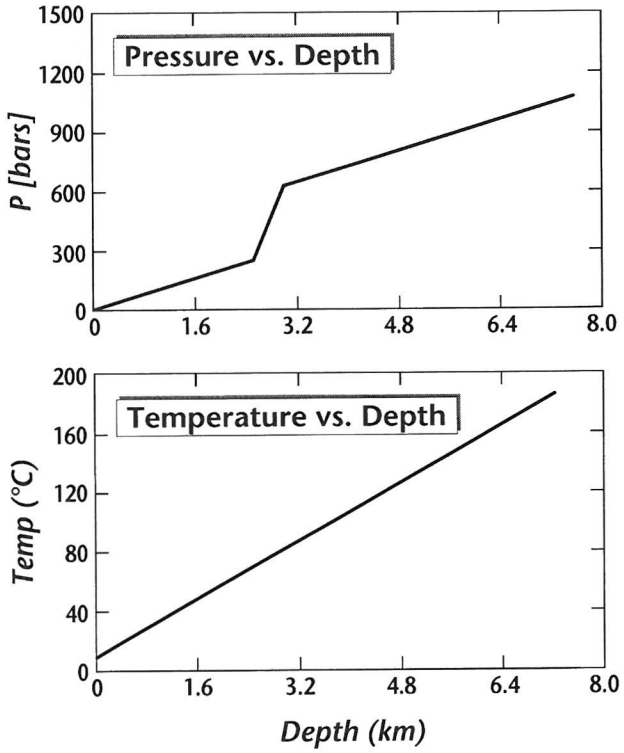

Figure 11. Pressure vs. depth and temperature vs. depth curves used in Figure 12.

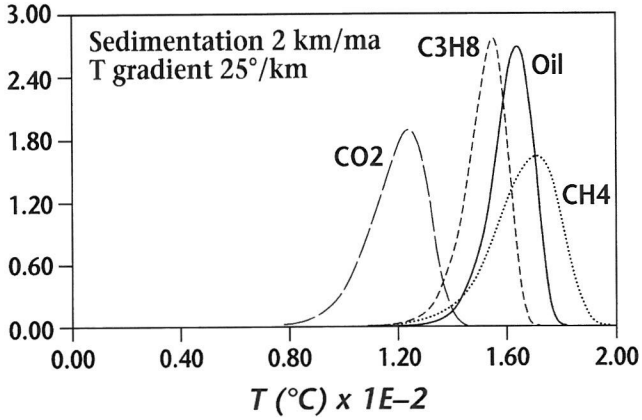

Figure 12. Calculated evolution of gas and oil as a function of depth, using breakdown scheme in Figure 12 and activation energies from Hunt et al. (1991) and Hunt and Hennet (1992). The Y axis represents the fraction of reaction that has gone to completion, $(dm_{ii}/m_i)/dt$, where m_{ii} is the ith product and t is time.

Figure 11. The kerogen maturation scheme in Figures 10 and 12 is based on experimental data from Ungerer et al. (1981, 1988) and data summarized in Hunt and Hennet (1992). The products were confined to dry gas, methane; one typical wet gas component, propane; and oil (Figure 10). It was further assumed that with further burial, residue R_1 can undergo further cracking to 0.15 g methane and 0.068 mg of a pyrobitumen residue, R_3. Reasonable activation energies and frequency factors for each of these reactions were estimated from the literature, as summarized in Hunt et al. (1991) and Hunt and Hennet (1992).

The first point we would make from Figures 10 and 12 is that even very low TOC rocks produce enough methane to saturate basin pore waters and produce a separate gas phase. Bonham (1978) shows that the solubility of methane in the overpressured parts of basins is ≈3000 to 14,000 ppm. But 0.2% TOC generates over 10,000 ppm methane in 10% porosity sediments of density 2 g/cc; 0.4 weight percent TOC sediments would generate 20,000 ppm methane. Methane that is generated in excess of that which can be dissolved in pore water will form a separate gas phase. The portion of the TOC value assumed to contribute separate phase reaction gas in Figure 13 is 0.2%. The total TOC of the sediments would be about 0.4%. The approximate average TOC value for all open-ocean sediments worldwide is about 0.2% (summarized in Calvert and Pedersen, 1992), a value about ten times lower than typically found for even a marginal quality petroleum source rock. But 0.4% TOC is typical of many intervals of the Weaver well (Figure 8 and Table 1). This value of TOC thus represents the minimum that could typically be expected from most rocks in most sedimentary basins, even those which are too organically lean to be considered as petroleum source rocks.

If we assume for the moment that all the gases in Figure 12 go into a separate gas phase and escape vertically, the vertical flux of gases out of the basin due to maturation of 0.2% kerogen sediments buried at 2 km/m.y. is shown in Figure 13. The flux was calculated for CH_4 and oil at the pressures and temperatures at the top of overpressure using the Behar et al. (1985) equation of state. Figure 13 shows that a flux of >1.4 liter/cm^2/ma of methane could be expected into the base of the oil window in a basin with 0.2 wt% TOC subsiding at 2 km/m.y.

The reason that this flux of CH_4 is interesting is that the solubility of oil-in-methane at pressures greater than 200 bars is very large. Figure 14 shows some of the solubility of oil in methane data found in experiments reported by Price et al. (1983). Referring to the solubility of oil in methane is misleading in one sense because oil and methane form a single mixed phase at the pressures and temperatures encountered in the deep parts of a basin. This single phase crosses a bubble curve at which a separate gas phase separates at about the depths at which pressure seals form. This process and its consequences will be discussed in a separate paper. Deep kerogen maturation produces a separate gas phase that becomes a gas/oil mixture as it dissolves oil generated higher in the basin. In the sense that this oil is dissolved in gas streaming from greater depths, the oil can be considered to be soluble in the gas.

The amount of oil that can be dissolved by methane along the P-T path of Figure 11 was measured directly by Price et al. (1983). Those data were

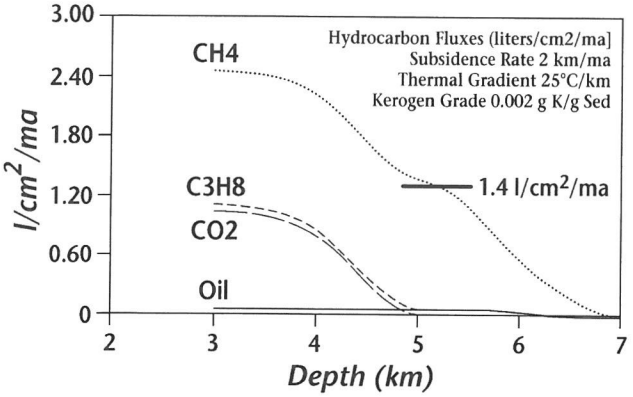

Figure 13. Calculated fluxes of gas and oil as a function of depth using kerogen breakdown scheme in Figure 11 and activation energies from Hunt et al. (1991) and Hunt and Hennet (1992). Volumes calculated at 87.5°C and 290 bars. ρCH4 = ρCO2 = 0.16, ρC3H8 = 0.49.

used to obtain the oil-in-methane "solubility" equation in Figure 14 and the curve shown in Figure 15. The curve is dashed below the depth at which the methane generated from a sediment of any particular kerogen grade (i.e., type and richness) can dissolve all of the oil generated in sediments of the same grade. Since the generative ratio is 0.67 g oil/g CH_4 (Figure 10), and CH_4 has a density of 0.66 g CH_4/liter at 25°C and 1 bar, the curve is dashed to: (0.67)(0.66) = 0.44 g oil/liter methane at STP. Price's experiments were carried out using a Spindle Top oil that is generally similar to oils from many other basins.

Figure 15 shows that gas streaming through a basin can mobilize oil upward but that there is a steep drop in the solubility of oil across the pressure transition zone where gas exsolves from the gas/oil mixture to produce separated oil and gas phases. Oil transported by the gas will be dumped out of the gas/oil phase going through the pressure transition at the top of the seal zone and become available to aid in the plugging process. Such a precipitation process is consistent with our observation of heavy oil, asphalt, or pyrobitumen in and around every seal zone observed to date. Note that in our calculations, the generative ratio of oil to gas is 0.44 g oil/liter CH_4, STP, so that at a uniform weight percent kerogen content in the sediments, all oil could be dissolved and moved upward to the end of the dashed line in Figure 15. The transport capabilities depend on the generative ratio and are the same for all kerogen concentrations. Thus, in either very organic lean rock, such as assumed in these calculations, or in very organic rich rocks, enough methane would be produced to carry oil generated below the seal zone up into the pressure transition zone.

The data of Price (1983) can also be used to estimate the composition of oil precipitated across selected 0.2 km depth intervals along the P-T curves of Figure 11, as shown in Figure 16. The average composition of oil dropped out at shallower depth above the

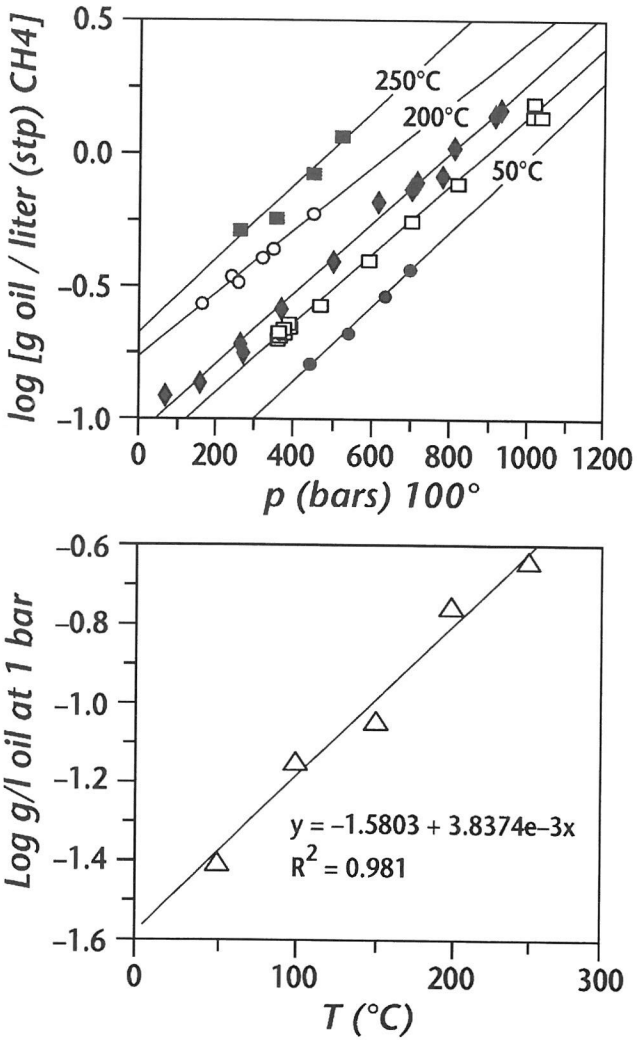

Figure 14. Solubility of oil in gaseous methane at P > 200 bar. Data from Price et al. (1983). Log Coil = −1.58 + 3.837 × 103 T (°C) + 1.3 × 10–3 P (bars).

seal, e.g. 2.2 km, has a maxima in average carbon numbers in the range of C_{12} to C_{18}, while the oils precipitated between 3 and 6 km (in and below the seal) tend to have more of the heavier carbon numbers. This change corresponds to observations in the Mix well (Figure 4) as well as in the pressure transition zone of a Mahakam Delta well (Vandenbroucke and Durand, 1981), where lighter hydrocarbon components predominate at the top of the seal while heavier components predominate at the bottom.

The oil precipitated within the pressure transition zone will also reduce the thermal conductivity of sediments, as shown in Figure 17. The points represent experimental thermal conductivities measured for quartz sand filled with air, oil, or brine with the lines representing the theoretical curves calculated by Cathles (unpublished results) based on series and parallel combinations of pore spaces filled with oil and/or air using fabric theory (Jowett et al., 1993). Both the experimental results (points on Figure 17) and theoretical calculations (lines and large circles)

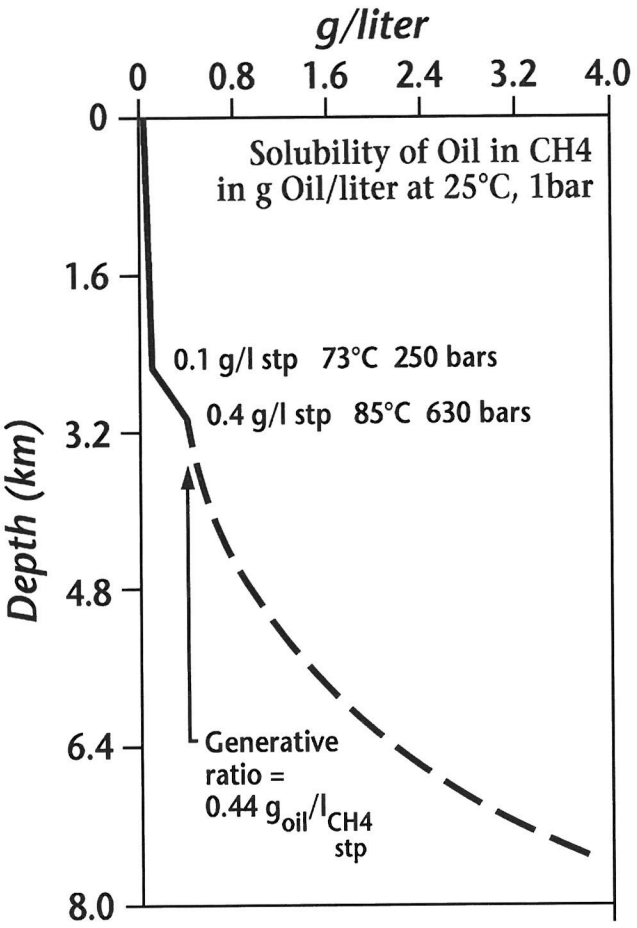

Figure 15. Methane in gas phase will mobilize oil to near top of geopressure.

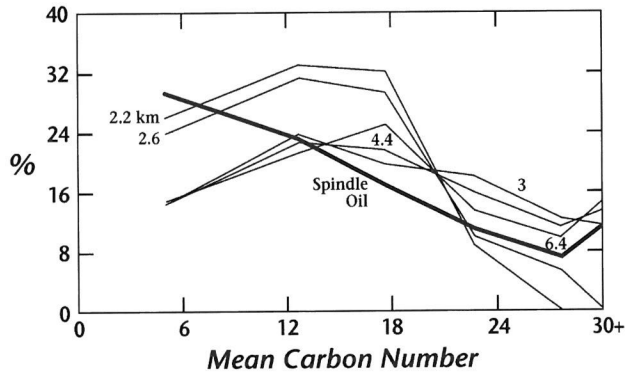

Figure 16. Expected composition of condensate oil dropped out of gas phase in passing depth indicated. Composition of start in Spindle Oil is shown by heavy line. Note predominance of lower carbon numbers in going from shallower depths. (Based on data from Price et al., 1983.)

show that filling pores with oil can halve the thermal conductivity observed when pores are filled with brine. Note that the presence of any free gas would decrease the thermal conductivity even further. The

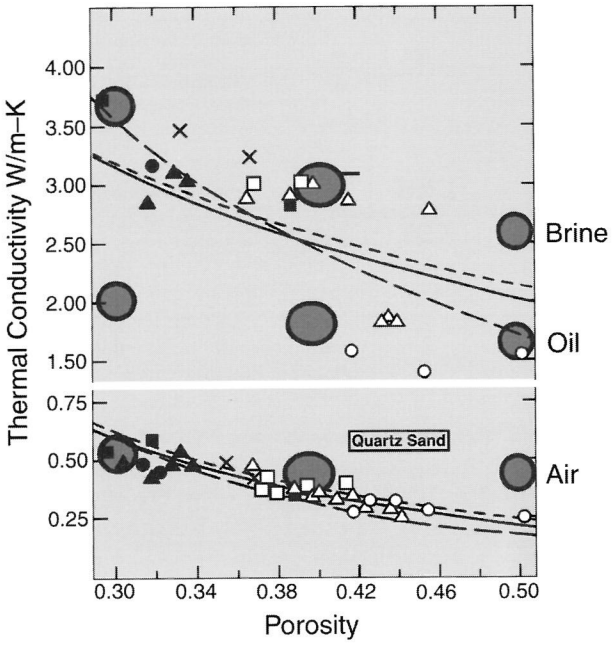

Figure 17. Calculated and experimentally observed effect of oil vs water in sediment pores on thermal conductivity.

decrease in thermal conductivity across the pressure transition zone is consistent with the higher thermal gradient in the pressure transition zone observed both by Jones (1975) and Engelder et al. (unpublished results) as part of this project, as well as the sharp change in vitrinite maturity gradient observed at the top of the pressure transition zones of the Gulf Coast Mix well (Figure 7), a weaker gradient for the Anadarko basin Weaver well (Figure 9), and possibly also for the Nova Scotia Venture Field H-22 well (Whelan and Eglinton, unpublished results).

The precipitation of polar and hydrocarbon constituents can plug intervals that already have low permeability due to their lithology, inorganic cementation, extreme compaction, or other factors. The plugging is a combination of heavy oil condensation and capillary effects that will be discussed in a subsequent publication. Inorganic mineral alteration constituents have a very low solubility in water (<0.1 wt.%) compared to the solubility of hydrocarbons in methane (66 wt.%) so that this oil condensation provides a comparatively effective mechanism for healing ruptured seals. The composition of the condensed oil through the pressure transition zone may record the status of gas and oil maturation and migration deeper in the basin.

CONCLUSIONS

The purpose of this research was to develop specific organic analyses that could aid in finding and characterizing pressure seals, particularly in shales where RFT measurements are not possible. In addition, we wished to gain some preliminary information on how sedimentary rock organic matter might be involved in

the formation and maintenance of pressure seals. Summarized below are the findings of this work with respect to each of these.

1. Determination of organic geochemical signatures diagnostic of pressure compartments and seals, as distinguished from those of similar normally pressured sedimentary rocks: (a) A zone of increase in vitrinite reflectance at the top of the pressure seal zone; organic petrographic evidence of bitumen maturation within the same zone. (b) Characteristic patterns of P_1 C_7–C_{16} hydrocarbon compositions above, within, and below the seal zone, including a progression of aliphatic n-alkanes from a predominance of the lighter nC_8 at the top of the seal to the heavier nC_{14} at the bottom; a piling up of all C_7 to C_{16} hydrocarbons just below the seal; and possibly a predominance of the aromatic compounds xylene and toluene above the seal. (c) A predominance of asphaltene and pyrobitumen over less-polar aliphatic and aromatic hydrocarbons in the vicinity of the seal zone. (d) Close association of asphaltene/micrinite with carbonate cementation, silicate dissolution and precipitation, and, sometimes, epigenetic pyrite phases in the vicinity of the seal zone. (e) Some preliminary evidence of microfractured quartz within and below seal zones.
2. Preliminary information on the effects pressure compartments and seals might have on oil and gas distributions in sedimentary rocks: see (b) and (c) above.
3. Preliminary research on how organic maturation and migration processes might be contributing to pressuring and sealing mechanisms (versus being parallel inorganic processes affected by the same time-temperature regime).

A plugging hypothesis is presented in which oil dissolved in upward-streaming gas is precipitated by the pressure drop across the seal zone. The precipitated bitumens plus the associated gas acting together with inorganic precipitation/cementation are postulated to produce a seal. This hypothesis accounts for the very low permeabilities observed in seals, the characteristic hydrocarbon distributions across the seals, the presence of a high proportion of heavy residual oil (i.e., asphalt and pyrobitumen) within and adjacent to the seal zone, and the increases in maturity observed within the seal. The hypothesis also takes into account the ability of the upward-streaming gas to aid in sealing. In cases of seal rupture, precipitation of heavy oil components in the seal would aid in subsequently healing the ruptures. The very tight association of carbonate cements, pyrite, asphaltene, and micrinite is strongly suggestive that the interaction of organic and inorganic reactions are important in seal formation and maintenance. Organic bitumen was observed to coat the quartz grains that were encased by a subsequent phase of secondary silica overgrowths in some samples from both the Mix and Weaver wells. This relationship indicates hydrocarbons had entered these intervals prior to secondary cementation. The presence of both mineral cements (calcite and silica) and organic asphalt-micrinite phases in the vicinity of seals suggests that inorganic cemented intervals interspersed with the organic matter might produce a seal more impermeable to passage of both aqueous and hydrocarbon fluids than either acting alone.

At the Mix well, the bottom of the seal zone occurs within the gas maturation window so that gas generation and pressure buildup could be contributing to the overpressuring of these sedimentary rocks, as proposed by Hedberg (1974) and discussed more recently by Barker (1987 and 1990) with the sealing being aided by the capillary gas pressure as proposed by Iverson et al., this volume.

Preliminary calculations show that very low TOC rocks (possibly as low as 0.2 to 0.5% TOC) may be capable of generating sufficient methane to form a separate hydrocarbon phase at depth. Because almost all sedimentary rocks, including nonsource rock open-ocean sedimentary rocks, contain at least these low amounts of TOC, the "hydrocarbon plugging" mechanism of seal formation could occur very widely both in petroleum and nonpetroleum source rock. An example of such a "low TOC" seal studied in this research may be a weak pressure transition zone in the Anadarko basin Weaver well.

ACKNOWLEDGMENTS

We thank Jeff Seewald, John Hunt, and Suzanne Weedman for careful reading of the manuscript and helpful discussions; Mary Zawoysky for editorial help; Carl Johnson for running GCMS analyses; Bob Nelson and Mary Zawoysky for carbon analyses; and our collaborators at Pennsylvania State University and Oklahoma State University, particularly Susan Weedman, Terry Engelder, and Vennessa Tigert for providing samples and background information as well as helpful discussion and encouragement. Help from Amoco, particularly John Bradley and Dave Powley, in initiating this research and in providing samples and background information is gratefully acknowledged. We thank the editor, Peter Ortoleva, for his help and patience during the preparation of this manuscript, and three anonymous reviewers for their careful reading of the manuscript and helpful suggestions. This work was supported by the Gas Research Institute, Contract Nos. 5088-260-1746 and 5091-260-2298. Woods Hole Oceanographic Institution Contribution No. 7984.

REFERENCES CITED

Barker, C., 1987, Development of abnormal and subnormal pressures in reservoirs containing bacterially generated gas: American Association of Petroleum Geologists Bulletin, v. 71, p. 1404–1413.

Barker, C., 1990, Calculated volume and pressure changes during the thermal cracking of oil to gas in reservoirs: American Association of Petroleum Geologists Bulletin, v. 74, p. 1254–1261.

Behar, E., R. Simonet, and E. Rauzy, 1985, A new non-

cubic equation of state: Fluid Phase Equilibria, v. 21, p. 237–255.
Bonham, L.C., 1978, Solubility of methane in water at elevated temperatures and pressures: American Association of Petroleum Geologists Bulletin, v. 62, p. 2478–2488.
Bradley, J.S., 1975, Abnormal formation pressure: American Association of Petroleum Geologists Bulletin, v. 59, p. 957–973.
Calvert, S.E. and T.F. Pedersen, 1992, Organic carbon accumulation and preservation in marine sediments: how is anoxia important? *in* J.K. Whelan and J.W. Farrington, eds., Organic Matter: Productivity, Accumulation, and Preservation in Recent and Ancient Sediments: New York, Columbia University Press, p. 231–263.
Clementz, D.M., 1979, Effect of oil and bitumen saturation on source-rock pyrolysis: American Association of Petroleum Geologists Bulletin, v. 63, p. 2227–2232.
Cooles, G.P., A.S. Mackenzie, and T.M. Quigley, 1986, Calculation of petroleum masses generated and expelled from source rocks: Organic Geochemistry, v. 10, p 235–245.
Creaney, S., 1980, The organic petrology of the Upper Cretaceous Boundary Creek formation, Beaufort-Mackenzie Basin: Bulletin of Canadian Petroleum Geology, v. 28, p.112–119.
Dembicki, H., Jr., B. Horsfield, and T.T.Y. Ho, 1983. Source rock evaluation by pyrolysis-gas chromatography: American Association of Petroleum Geologists Bulletin, v. 67, p 1094–1103.
Durand, B., 1988, Understanding of hydrocarbon migration in sedimentary basins (present state of knowledge): Organic Geochemistry, v. 13, p 445–459.
Espitalié, J., 1986, Use of T_{max} as a maturation index for different types of organic matter. Comparison with vitrinite reflectance, *in* J. Burrus, ed., Thermal Modeling in Sedimentary Basins: Paris, Editions Technip, p. 475–496.
Espitalié, J., F. Marquis, and I. Barsony, 1984, Geochemical logging, *in* K.J. Voorhees, ed., Analytical Pyrolysis: Boston, Butterworths, p. 276–304.
Espitalié, J., J.L. LaPorte, M., Madec, F. Marquis, P. Leplat, J. Paulet, and A. Boutefeu, 1977, Méthode rapide de caractérisation des roches méres de leur potentiel pétrolier et de leur degré d'evolution: Reviews de l'Institute Francais du Pétrol., v. 32, p. 23–42.
Hedberg, H., 1974, Relation of methane generation to undercompacted shales, shale diapirs, and mud volcanoes: American Association of Petroleum Geologists Bulletin, v. 58, p. 661–673.
Horsfield, B., 1984, Pyrolysis studies and petroleum exploration, *in* J. Brooks and D. Welte, eds., Advances in Petroleum Geochemistry, v. 1: London, Academic Press, p. 247–298.
Huc, A.Y., and J.M. Hunt, 1980, Generation and migration of hydrocarbons in offshore South Texas Gulf Coast sediments: Geochimica et Cosmochimica Acta, v. 44, p. 1081–1089.
Hunt, J.M., 1979, Petroleum Geochemistry and Geology: San Francisco, Freeman, 617 pp.
Hunt, J.M., 1985, Generation and migration of light hydrocarbons: Science, v. 226, p. 1265–1270.
Hunt, J.M., 1990, Generation and migration of petroleum from abnormally pressured fluid compartments: American Association of Petroleum Geologists Bulletin, v. 74, p. 1–12.
Hunt, J.M., and R. J-C Hennet, 1992, Modeling petroleum generation in sedimentary basins, *in* J.K. Whelan and J.W. Farrington, eds., Organic Matter: Productivity, Accumulation, and Preservation in Recent and Ancient Sediments: New York, Columbia University Press, p. 20–51.
Hunt, J.M., M.D. Lewan, and R. J-C. Hennet, 1991, Modeling oil generation with time-temperature index graphs based on the Arrhenius equation: American Association of Petroleum Geologists Bulletin, v. 75, p. 795–807.
ICCP (International Committee for Coal Petrology), 1963, 1971, 1975, International Handbook of Coal Petrography, Paris, CNRS.
Jacob, H., 1989, Classification, structure, genesis and practical importance of natural solid oil bitumen ("migrabitumen"): International Journal of Coal Geology, v. 11, p. 65–79.
Jansa, L.F., and Norguera, V., 1990, Geology and diagenetic history of overpressured sandstone reservoirs, Venture Gas Field, offshore Nova Scotia, Canada: American Association of Petroleum Geologists Bulletin, v. 74, p. 1640–1658.
Jones, P.H., 1975, Geothermal and hydrocarbon regions, Northern Gulf of Mexico Basin, *in* M.H. Dorfrom and R.U. Deller, eds., Proceedings First Geopressured Energy Conference, Center for Energy Studies, University of Texas at Austin, p. 15–97.
Jowett, E.C., L.M. Cathles, and B.W. Davis, 1993, Predicting depths of gypsum dehydration in evaporitic sedimentary basins: AAPG Bulletin, v. 77, p. 402–413.
Karlsen, D., and S.R. Larter, 1991, Analysis of petroleum fractions by TLC-FID: applications to petroleum reservoir description: Organic Geochemistry, v. 17, p. 603–617.
Larter, S.R., 1984, Application of analytical pyrolysis techniques to kerogen characterization and fossil fuel exploration/exploitation, *in* K.J. Voorhees, ed., Analytical Pyrolysis Techniques and Explorations: London, Butterworths, p. 212–275.
Lewan, M.D., 1987, Petrographic study of primary petroleum migration in the Woodford Shale and related rock units, *in* B. Doligez, ed., Migration of Hydrocarbons in Sedimentary Basins: Paris, Edition Technip, p. 113–130.
Leythaeuser, D., H.W. Hagemann, A. Hollerbach, and R.G. Schaefer, 1980, Hydrocarbon generation in source beds as a function of type and maturation of their organic matter: a mass balance approach: Tenth World Petroleum Congress Proc., v. 2, p. 31–41.
Mukhopadhyay, P.K., 1992, Maturation of organic

matter as revealed by microscopic methods: applications and limitations of vitrinite reflectance, and continuous spectral and pulsed laser fluorescence spectroscopy, *in* K.H. Wolf and G.V. Chilingarian, eds., Diagenesis, III. Developments in Sedimentology: Elsevier Science Publishers, New York, v. 47, p. 435–510.

Mukhopadhyay, P.K., and J.A. Wade, 1990, Organic facies maturation of sediments from three Scotian Shelf wells: Bulletin of Canadian Petroleum Geology, v. 38, p. 407–425.

Peters, K.E., 1986, Guidelines for evaluating petroleum source rock using programmed pyrolysis: American Association of Petroleum Geologists Bulletin, v. 70, p. 318–329.

Powley, D.E., 1980, Pressures, normal and abnormal: AAPG Advanced Exploration Schools Unpublished Lecture Notes, Tulsa, OK, American Association of Petroleum Geologists, 38 p.

Powley, D.E., 1990, Pressures and hydrogeology in petroleum basins: Earth-Science Reviews, v. 29, p. 215–226.

Price, L.C., L.M. Wenger, T. Ging, and C.W. Blount, 1983, Solubility of crude oil in methane as a function of pressure and temperature: Organic Geochemistry, v. 4, p. 201–221.

Stach, E., Mackowsky, M Th., Teichmüller, M., Taylor, G.H., Chandra, D., and Teichmuller, R., 1982, Textbook of Coal Petrology: 3rd ed.: Gebrüder Borntraeger Berlin, Stuttgart, 535 pp.

Tarafa, M.E., J.K. Whelan, and J.W. Farrington, 1988, Investigation on the effects of organic solvent extraction on whole-rock pyrolysis: Multiple-lobed and symmetrical P2 peaks: Organic Geochemistry, v. 12, p. 137–149.

Thompson, K.F.M., 1979, Light hydrocarbons in subsurface sediments: Geochimica et Cosmochimica Acta, v. 43, p. 657–672.

Thompson, K.F.M., 1988, Gas-condensate migration and oil fractionation in deltaic systems: Marine and Petroleum Geology, v. 5, p. 237–246.

Tigert, V., and Z. Al-Shaieb, 1990, Pressure seals: their diagenetic banding patterns: Earth-Science Reviews, v. 29, p. 227–240.

Tissot, B. P., and D.H. Welte, 1984: Petroleum Formation and Occurrence: Berlin, Springer-Verlag, 609 p.

Ungerer, P., E. Behar, and D. Discamps, 1981, Tentative calculation of the overall volume expansion of organic matter during hydrocarbon genesis from geochemistry data. Implication for primary migration: Advances in Organic Geochemistry: New York, Wiley, p. 129–135.

Ungerer, P., E. Behar, M. Villalba, O.R. Heum, and A. Audibert, 1988, Kinetic modelling of oil cracking: Organic Geochemistry, v. 13, p. 857–868.

Vandenbroucke, M., and B. Durand, 1983, Detecting migration phenomena in a geological series by means of C1–C35 hydrocarbon amounts and distributions: Advances in Organic Geochemistry: New York, Wiley, p. 147–155.

Weedman, S.D., A.L. Gruber, and T. Engelder, 1992, Pore pressure variation within the Tuscaloosa Trend: Morganza and Moore-Sams Fields, Louisiana Gulf Coast: Journal of Geophysical Research, v. 97, p. 7193–7202.

Whelan, J.K., J.M. Hunt, and A.Y. Huc, 1980, Applications of thermal distillation-pyrolysis to petroleum source rock studies and marine pollution: Journal of Analytical and Applied Pyrolysis, v. 2, p. 79–96.

Whelan, J.K., J.M. Hunt, J. Jasper, and A. Huc, 1984, Migration of C_1–C_8 hydrocarbons in marine sediments: Organic Geochemistry, v. 6, p. 683–694.

Whelan, J.K., J.W. Farrington, and M.E. Tarafa, 1986, Maturity of organic matter and migration of hydrocarbons in two Alaskan North Slope wells: Organic Geochemistry, v. 10, p. 207–219.

Whelan, J.K., Z. Kanyo, M. Tarafa, and M.A. McCaffrey, 1990, Organic matter in Peru Upwelling sediments-analysis by pyrolysis, pyrolysis-gas chromatography, and pyrolysis-gas chromatography–mass spectrometry, *in* E. Suess, R. von Huene et al., eds., Proceedings of the Ocean Drilling Program, Scientific Results, College Station, TX, v. 112, p. 573–590.

Basin Compartments and Seals

Edited by

Peter J. Ortoleva

Department of Chemistry
Indiana University
Bloomington, Indiana

AAPG Memoir 61

Published by
The American Association of Petroleum Geologists
Tulsa, Oklahoma, U.S.A.
Printed in the U.S.A.

1994